Winter Lightning and Heavy Frozen Precipitation in the Southeast United States

S. M. HUNTER*

NOAA/National Weather Service, Dodge City, Kansas

S. J. UNDERWOOD+

Department of Geography, California State University, Fresno, California

R. L. HOLLE#

National Severe Storms Laboratory, Norman, Oklahoma

T. L. MOTE

Department of Geography, University of Georgia, Athens, Georgia

(Manuscript received 26 June 2000, in final form 22 February 2001)

ABSTRACT

This study addresses winter season lightning by examining synoptic-scale circulations, cloud-to-ground (CG) lightning patterns, and frozen precipitation. Specifically, locations, frequencies, and polarities of CG flashes are related to the location, intensity, and type of heavy frozen precipitation (snow, freezing rain, or ice pellets) for seven winter storms affecting the southeast United States from 1994 through 1997. The results suggest two distinct phases of winter storm development, each producing different patterns of CG lightning and frozen precipitation. These phases are termed the arctic front (AF) and migratory cyclone (MC) types.

Analysis was performed on 27 periods within the seven cases. In several periods, there were significant numbers of CG flashes within or near a subfreezing surface air mass and frozen precipitation when a quasi-stationary arctic front existed. These periods were classified as AF phases. This flash pattern indicates a connection between the intensity of convection (associated with CG flashes) and downwind frozen precipitation. In these situations there was strong southwesterly flow aloft, which may have advected ice particles from these convective clouds into stratiform clouds near the frontal surface. This process resembles the ''seeder–feeder'' mechanism of precipitation growth.

The AF phases eventually developed into MC phases, and the latter were more common in this study. The MC phases in general exhibit a different spatial relationship between CG lightning and heavy frozen precipitation; that is, CG flashes retreat toward the warm sector of the cyclone and thus are not proximal to the 0°C surface isotherm. There appears to be little connection between convection and frozen precipitation in most of these situations. The distinction between AF and MC phases, in conjunction with CG lightning monitoring, may aid forecasts of the duration and amount of frozen precipitation during winter storms.

1. Introduction

Winter storms producing significant frozen precipitation (snow, freezing rain, or ice pellets) across the southeastern United States are not as common as in other areas of the country and, probably for that reason, have been less analyzed in the literature. Despite this modest frequency, these storms and their frozen precipitation can disrupt human activity in the region (Rooney 1967). Heavy snowfalls in the Southeast have been analyzed and composite synoptic conditions favorable for their development have been identified (Mote et al. 1997). Synoptic and dynamic processes favorable for heavy snowfall have also been examined for other regions of the country (Uccellini and Kocin 1987; Kocin and Uccellini 1990; Kocin et al. 1995). There are, however, limitations to forecasting/nowcasting complex winter precipitation and convection across the southeast and mid-Atlantic United States. This complexity is the result, in part, of the topography of the region and the

* Current affiliation: U.S. Bureau of Reclamation, Denver, Colorado.

+ Current affiliation: Department of Geography, Southern Illinois University, Carbondale, Illinois.

Current affiliation: Global Atmospherics, Inc., Tucson, Arizona.

Corresponding author address: Steven M. Hunter, U.S. Bureau of Reclamation D-8510, Denver Federal Center, P.O. Box 25007, Denver, CO 80225-0007.
E-mail: smhunter@do.usbr.gov

prevalence of Appalachian cold air damming during the winter months (Keeter and Cline 1991). The potential of cloud-to-ground (CG) lightning detection networks to augment existing radar, radiosonde, and satellite technologies in forecasting and nowcasting frozen precipitation has been the subject of almost no research. Such augmentation seems viable, however, since the southeast United States has adequate CG lightning detection network coverage (Cummins et al. 1998) and a higher incidence of cool season convection than other U.S. regions. At the very least, near–real time lightning flash data should be useful for detecting the initiation, existence, or trend of winter season convection, identifying embedded convection, and diagnosing moist symmetric instability (MSI).

Climatological analyses of winter lightning have identified flash density maxima over the Gulf Stream off the east coast (Orville 1990) and the central United States (Holle and Cortinas 1998). Moore and Idone (1999), using CG data from six winters, found that only 0.55% of total flashes occurred within subfreezing surface air. The majority of these flashes occurred in the central and south-central United States, similar to Holle et al. (1998). Of the few studies of lightning in winter, most have focused on single storms. Holle et al. (1997) analyzed a single isolated flash that destroyed a Connecticut home in February. Schultz (1999) explored lake-effect snowstorms in Utah and New York in an attempt to determine those parameters capable of discriminating storms with lightning from those without lightning. Orville (1993), Bradshaw (1994), and Dickinson et al. (1997) examined the ''Superstorm of '93,'' which produced prodigious CG lightning in its warm sector. Roohr and Vonder Haar (1996) found heavy snow downstream of lightning clusters during a March storm in Colorado. Studwell and Orville (1995) studied lightning patterns in a severe ice- and snowstorm over the Southeast and Atlantic coast. They discovered a predominance of positive flashes (delivering net positive charge to ground) in areas of freezing rain. A similar association was made by Holle and Watson (1996) for two central U.S. events. High positive flash percentages have also been reported for a variety of locations and storm types (Brook et al. 1982; Williams 1988; Goto et al. 1992; Orville 1993).

This research will address some of the shortcomings in the current knowledge of winter lightning, by documenting the primary atmospheric processes that accompany such lightning across the southeast United States. Our initial hypothesis was that a relationship exists between convection and downwind heavy frozen precipitation. The study therefore focuses on processes resulting in cold season convection. There is a diagnosis of the meteorological environment of the lightning-producing winter storms, particularly regarding vertical stability and motions, in the hope that predictive tools for those storms may result. Finally, the research investigates relationships of lightning flash density and polarity with location, intensity, duration, and phase of winter precipitation.

2. Case studies and methodology

a. Motivation for and selection of case studies

A case study approach was chosen for several reasons. First, the number of major winter storms in the southeast United States since the advent of operational CG lightning data has been inadequate to construct a representative climatological or composite study. Even if compositing were possible, it would yield a picture that obscures details through averaging. This result is undesirable, as the study is designed to extract such details from the relationships between lightning and synoptic-scale weather. We were able to identify seven cases for study, however. This is a sufficiently large sample to hint at the climatological character of such storms, since the total winter storm population in the Southeast is comparatively small.

The seven cases were selected based on several factors. First, the cases involved winter storms with major societal impacts to the Southeast, owing to heavy frozen precipitation. These impacts were determined from state-by-state entries in *Storm Data*, gathered by National Weather Service (NWS) offices and published monthly by the National Climatic Data Center in Asheville, North Carolina. Four of the cases have been the subject of prior research. Second, the cases were all after the 1993/94 winter, the first winter with upgraded National Lightning Detection Network (NLDN; Cummins et al. 1998) detection efficiency and accuracy. Finally, although all storms were known to produce CG flashes, their storm-relative locations and extents were largely unknown at the time of their initial identification. This circumstance meant that there was no predilection toward certain lightning/precipitation configurations in the cases' selection, so that they might be representative of the larger population of winter storms with lightning in the southeast United States. There may be snow- or icestorms in the Southeast without significant CG lightning, but these are not included in this study.

The characteristics and impacts of each case are summarized in Fig. 1. The domain encompassed by these impacts, which is mapped in Fig. 2, ranged from 30°–46°N and 75°–100°W. This domain encloses maxima in the climatological frequency of thunderstorms near- and below-freezing surface temperatures (Holle and Cortinas 1998; Moore and Idone 1999).

b. Synoptic, precipitation, and CG lightning analyses

The first component of the methodology consisted of a synoptic analysis of each case. The duration of a case was specified on the basis of impact times from *Storm Data*, that is, those periods with significant frozen precipitation. Synoptic-scale vertical motion that produced

Case, place, and date	Storm precipitation and impacts	Dominant lifting mechanisms; synoptic and cold air features
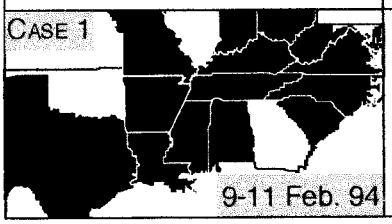	$300 million ice storm; up to 15 cm ice accumulation	Isentropic lift over shallow *arctic* airmass and upper divergence associated with jet; possible MSI/ frontogenesis
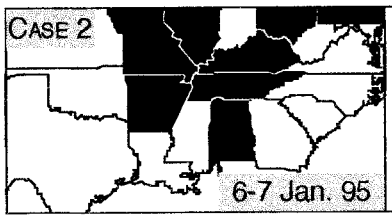	Freezing rain up to 2 cm accumulation; ice pellets	General isentropic upglide and strong warm air advection ahead of rapidly moving and well-developed cyclone
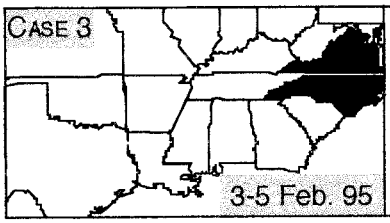	Mainly heavy snow up to 18 cm accumulation; some ice pellets	Isentropic lift/warm conveyor belt ahead of deepening migratory cyclone, combined with upslope flow into Appalachian range; some cold air damming in lee of range
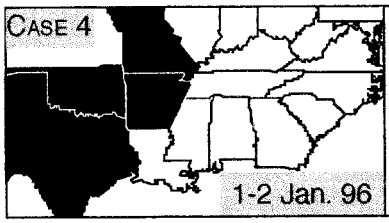	Exclusively heavy snow up to 30 cm	Migratory cyclone lifting with local enhancement by upslope flow in Ozarks; just enough cold air for snow in northwest cyclone quadrant
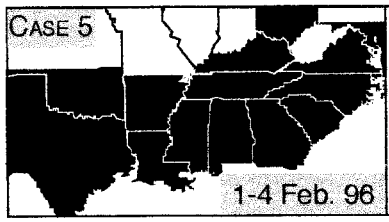	Widespread heavy ice up to 15 cm and snow up to 60 cm; multimillion dollar damage	Upper divergence associated with jet stream(s) and isentropic lift over *arctic* stationary front and frontogenetic circulations
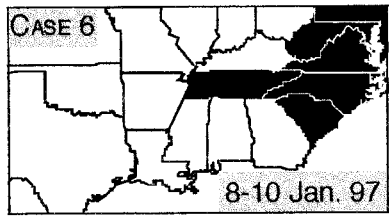	Freezing rain and/or ice pellets up to 8 cm; snow up to 15 cm	Strong isentropic upglide jet over dammed cold air in mid-Atlantic states. Impact area between complex deepening cyclone in Midwest and coastal low
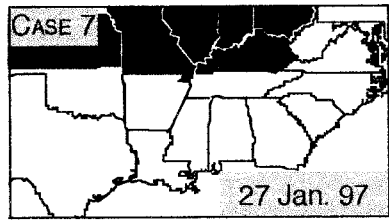	Heavy snow up to 20 cm and freezing rain up to 5 cm accumulation	Isentropic lift over strong east-west *arctic* front and circulations associated with upper jets and/or frontogenetic circulations

FIG. 1. States affected (shaded black), dates, precipitation impacts, and characterization of predominant lifting mechanisms and cold air involvement for numbered case studies.

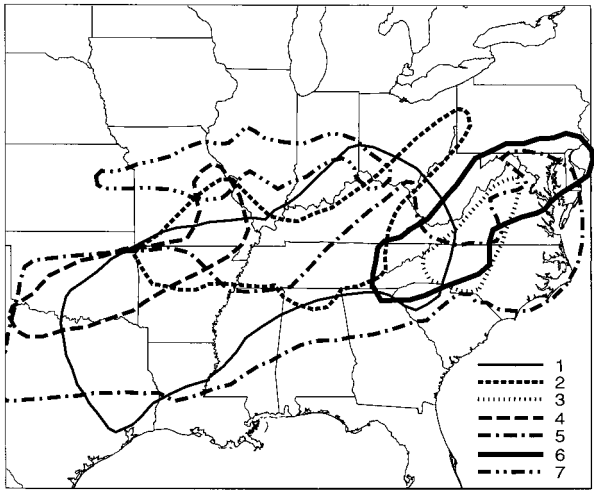

FIG. 2. Map of areas impacted by heavy frozen precipitation for seven cases in this study. Legend shows line style outlining impact polygons for each case. Impact areas are largely defined by *Storm Data* reports for entire precipitation event.

precipitation, particularly the frozen variety, was diagnosed using upper air and model data. This was initially done in cursory fashion with the aid of the National Oceanic and Atmospheric Administration's *Daily Weather Maps* series and a knowledge of typical winter storm patterns in the eastern United States (e.g., Gurka et al. 1995; Mote et al. 1997). Further analysis included a stability assessment, both moist symmetric and gravitational. Soundings and model data were inspected for this purpose. The model data were analyzed with the personal computer program PCGRIDDS. Nearly all such data were from the Eta Model initialization. Convection that was supported by instability, either slantwise or upright, was given emphasis in the analysis of vertical motion. This is because of convection's smaller horizontal scale and its prominence in production of lightning, which is addressed in the second component of the case analyses (lightning and precipitation).

The lightning examination focused on the location and frequency of CG flashes relative to the cold air mass and frozen precipitation. This was accomplished using mosaics of Weather Surveillance Radar-1988 Doppler images for precipitation estimation and CG locations and polarities from the NLDN. The total flashes and percent positive were calculated for areas within approximately 100 km on either side of the surface freezing line. We termed this the *buffer zone.* This was an attempt to isolate only those flashes that, with advection, could have affected the frozen precipitation. To further this endeavor, within-zone flash statistics were compared to similar computations for the entire flash domain. This domain included nearly all flashes in the southeast quadrant of the United States, occasionally extending into the northeast quadrant if significant numbers of flashes occurred there.

The surface freezing isotherms were taken from *Daily Weather Maps* for 1200 UTC and from Eta Model initializations of temperature at 1000 mb for 0000 UTC. Initially, flash calculations matching this temporal resolution were attempted, that is, across 12-h periods. This approach proved unsatisfactory, however, because during such periods surface features moved so much that the position of flashes relative to them lost meaning. It was decided instead to make flash calculations for 6-h periods, centered on the times of the surface freezing isotherm positioning. This approach yielded 27 such periods for the seven cases. These calculations allowed comparison between different phases within the same case and across cases (defined in section 3b) and led to stratification based on the nature of the surface cyclone, the freezing line position, and the position of CG flash clusters relative to those features. These techniques will be elaborated in subsequent sections.

3. Synoptic patterns

a. Upper troposphere

During the seven events analyzed in this study, there were several similarities in upper-tropospheric circulation features. In each of the seven cases, upper-tropospheric wind speed maxima were located eastward of 100°W longitude and originated near 30°N latitude. These maxima stretched to the northeast and often pushed off the mid-Atlantic coast. The trough axis of the 300-mb flow for the seven cases consistently migrated into eastern Texas and, in cases 1 and 3, well into the Gulf of Mexico. Six of the seven cases showed evidence of a split flow pattern, either before or during the frozen precipitation event. That is, the observed upper flow featured a separation of the polar jet into two distinct branches, northern and southern. In five of the six split flow cases, the branches phased into a single jet prior to the end of the precipitation event (hereafter referred to as a phased pattern). This merging of branches was probably the result of system maturation. The frequent presence of a southern branch jet with strong southwesterly flow suggests that it is very important to precipitation development. A southwesterly flow jet was found to be ubiquitous during winter thunderstorm outbreaks by Holle and Cortinas (1998). The southern jet probably promotes upper-tropospheric divergence that supports vertical motion for cyclone development in the region. Uccellini and Kocin (1987) demonstrated that ageostrophic circulations of distinct jet streaks can couple, invigorating vertical motion in the area of that coupling. Examination of such circulations with model initialization data revealed that only one case (case 7) showed evidence of coupling of the northern and southern branches of the polar jet.

Middle-tropospheric patterns at 500 mb were perused for each of the 27 periods encompassed by the seven cases. While too lengthy to describe each period, some patterns emerged. Not surprisingly, each of the seven

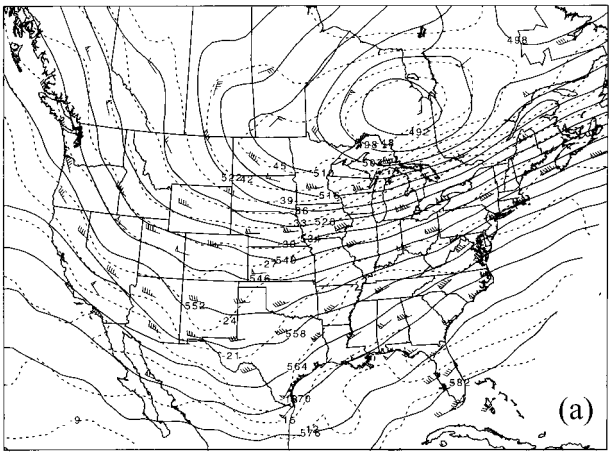

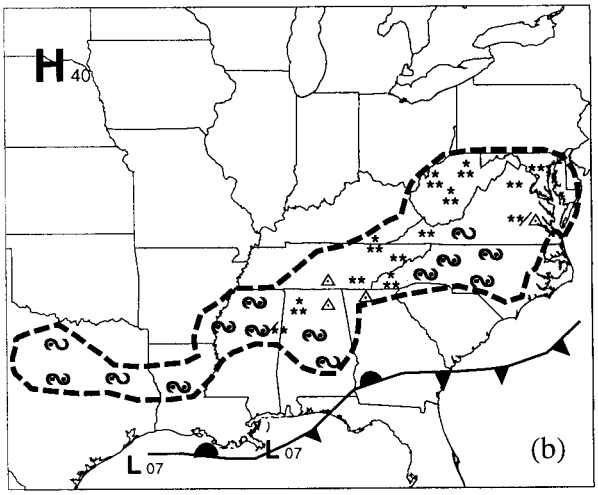

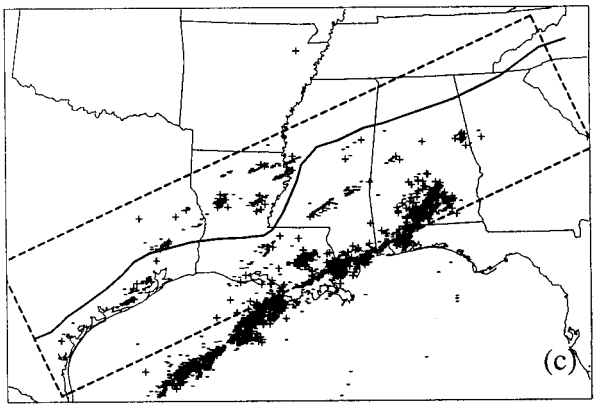

FIG. 3. (a) North American upper air chart for 500-mb level at 1200 UTC 2 Feb 1996 (case 5). Solid curved lines are geopotential heights in 60-gpm increments. Dashed curves are isotherms in 3°C increments. Wind barbs are standard, with a pennant representing approximately 50 kt; full barb, 10 kt, and half barb, 5 kt. Extracted from NOAA *Daily Weather Maps.* (b) Surface frontal and frozen precipitation analysis for 1200 UTC 2 Feb 1996. Stationary front maintained approximately the depicted location during the day of 2 Feb. Principal low pressure centers are denoted by an L with the last two digits of their central pressures shown adjacent; similar notation is used for anticyclone (H). Thick dashed polygon encloses the significant frozen precipitation extent for 2 Feb only. Precipitation symbols are standard and portray the predominant type of frozen precipitation in an area. (c) The CG flash locations from 0900 to 1500 2 Feb 1996 (midpoint time 1200 UTC). Dashes represent CGs delivering negative charge to ground; plus signs, CGs delivering positive charge. Curved line is position of surface freezing line at midpoint time. Dashed trapezoid outlines an area approximately 100 km on either side of this line, defining a buffer zone for flash calculations (see section 2b). This period was characterized as an AF phase.

FIG. 3. (*Continued*)

cases exhibited some form of troughing. The cases differed in both the amplification of the trough and the position of the trough axis; the following descriptions refer to the *onset* of the heaviest precipitation. Cases 3 and 4 exhibited phased high-amplitude troughs, with extents from Ontario to the Gulf of Mexico and from Kansas to northern Mexico, respectively. Case 5 had a much broader phased trough across nearly the entire continental United States, with at least one embedded low-amplitude short-wave trough near the Rio Grande river basin (Fig. 3a). Case 6 also had a phased jet stream at the time of precipitation onset (Fig. 4a). During onset time, however, cases 1, 2, and 7 featured split flow, in which were embedded short-wave troughs of varying amplitude. The extents of these troughs ranged from Kansas to northern Mexico, and were more consistent in longitude than in the phased trough cases. There appeared to be no consistent distinction in upper-tropospheric patterns between arctic front (AF) and migratory cyclone (MC) phases (defined in the next subsection).

b. Lower troposphere and surface

The upper-tropospheric jet streaks discussed in the last subsection were associated with baroclinity and lower-tropospheric jets that advected warm moist air from the Gulf of Mexico over a cold air mass, resulting in isentropic upglide and supporting convection. The areas affected by heavy frozen precipitation were ahead of the surface low position (to the east or northeast) in all but cases 3 and 4, reflecting the importance of such jets and isentropic lift to this precipitation. This importance was also emphasized by Mote et al. (1997).

Lower-tropospheric conditions were similar in cases 1, 3, 4, and 6. Predominant flow at 850 mb was strong from the south. In each of these cases, before the onset of frozen precipitation, specific humidity levels indicated that a plume of moisture was in place across the southern Gulf states and as far north as Tennessee and Virginia. Case 7 also had at 850 mb a moisture plume and jet streak, but both were oriented southwest to northeast. Moreover, the cores of both features were displaced farther north and west (across western Louisiana, eastern Texas, and central Arkansas) than in cases 1, 3, 4, and 6. Cases 2 and 5 had 850-mb flow that was predominantly westerly across the study area, and humidity levels were slightly lower compared to the aforementioned cases.

The surface environment across the seven cases was

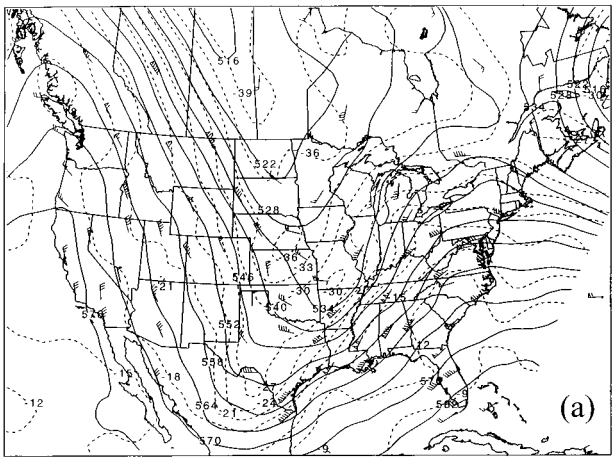

FIG. 4. Similar to Fig. 3 except for a midpoint time of 1200 UTC 9 Jan 1997 (case 6). Also, in (b) the long dashed line is track of the principal surface low (large L) during the 24 h centered on this time (with times noted at the end points). Second L in Georgia locates a weaker, coastal low. This period was characterized as an MC phase.

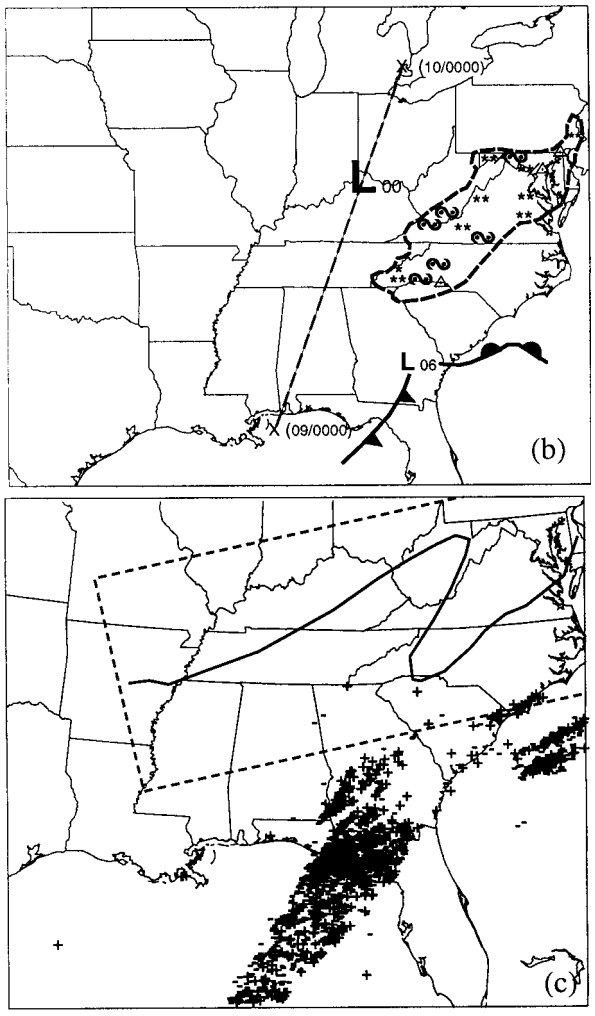

FIG. 4. (*Continued*)

analyzed by dividing their combined durations into 27 periods, each 12 h in duration. The periods were stratified into two *phases*, according to the nature of the main surface low pressure center or cyclone. This low was a region of cyclogenesis, a trough, or a quasi-stationary wave on an arctic front. When the surface situation was dominated by a quasi-stationary arctic front, the phase was called an arctic frontal phase. When a deep, mature, migratory cyclone was the primary surface feature, the phase was termed an MC type. The type of low that defined the phases had a profound effect on the distribution and intensity of frozen precipitation generated (Fig. 1, last two columns). Cases 1, 5, and 7 had AF phases. Note from the maps in Fig. 1 that precipitation impact areas in these cases were more widespread. In each MC phase of the study, areas affected by heavy frozen precipitation were in advance of the surface low position.

The surface expressions of each AF phase exhibited an east–west boundary at the leading edge of a large anticyclone. Low pressure associated with the AF was usually weak and collocated with the surface frontal boundary. Localized depressions developed in these phases, constituting waves on the front. The east–west thermal boundaries of the AF phases sharply contrast with the S-shaped, southwest–northwest orientation of the boundaries near mature MCs. The AF phases were found to produce heavier and more damaging frozen precipitation (Fig. 1, column 2), owing principally to ascent associated with a strong southwesterly jet streak atop an east–west frontal boundary plus slow movement of the low-level system.

A graphical description of the synoptic and lightning patterns for each period would be prohibitively long. Instead, two periods that typify the AF and MC phases were selected, each illustrated by the schematics in Figs. 3 and 4, respectively. Note the widespread frozen precipitation area in the AF phase, oriented parallel to and north of the arctic front (Fig. 3b). Contrast this with the MC phase, whose precipitation has little connection with any fronts and is confined to an area of cold air damming east of the Appalachian Mountains (Fig. 4b). The cold and warm fronts to the south of the precipitation area in this case were associated with a weak coastal low in Georgia and had little influence on the frozen precipitation area.

Table 1 categorizes the cyclone and frontal configurations for each period. The primary information in the table is the designation of periods into AF or MC phases (column five). Column four contains the 12-h translation distance of the dominant surface low, centered on the time in the second column. The AF periods are generally associated with smaller [$<$600 km (12 h)$^{-1}$] translations, as would be expected for waves forming on a front. An exception is the large motion for the first period in case number 7. This motion is misleading,

TABLE 1. Summary of lightning–freezing line separation, surface low center translation, and other characteristics for every period embraced by the seven cases. Translation period for surface low is 12 h centered on given time.

Case (year)	Period center time (UTC) and date	Lightning–freezing line separation[a]	Surface low translation (12 h, in km)	Comments
1 (1994)	0000[b] 10 Feb	Small	285	AF
	1200[b] 10 Feb	Overlapping/small	270	AF
	0000[b] 11 Feb	Medium	550	AF to MC
	1200 11 Feb	Medium to large	504	MC
2 (1995)	0000 6 Jan	Large	945 (cyclogenesis)	Lightning in SW United States, far from impact area
	1200 6 Jan	Overlapping/small	875	MC
	0000 7 Jan	Medium	1215	MC; accelerated migration
	1200 7 Jan	Large to SE	1065	MC
3 (1995)	0000 4 Feb	Medium to large	675	MC; deepening low entire case
	1200 4 Feb	Small to medium; most flashes in Gulf Stream	435	MC with moderate migration speed
	0000 5 Feb	Large	465	MC with moderate migration speed
4 (1996)	1200 1 Jan	Large	565	MC
	0000 2 Jan	Large	485	MC but slow migration
	1200 2 Jan	Medium to large	605	MC
	0000 3 Jan	Medium to large	775	MC; fast migration
5 (1996)	0000[b] 2 Feb	Tremendous overlap	75	AF; wave in Gulf
	1200[b] 2 Feb	Strong overlap	545	AF
	0000 3 Feb	Medium; few overlap	1345	MC
	1200 3 Feb	Medium	1510	MC; extremely fast migration (offshore)
	0000 4 Feb	Lightning well off coast at 1200 UTC 3 Feb	?	MC; low S of Nova Scotia by 1800 UTC 3 Feb but snow in S MD, SE VA, NW SC
6 (1997)	1200 8 Jan	Medium to large	400 (cyclogenesis)	Wave in Gulf; impact starts 1800 UTC 8 Jan in SC
	0000 9 Jan	Medium	765	MC; early migration
	1200 9 Jan	Large	820	MC; rapid migration
	0000 10 Jan	Very large	450	MC; deepening and slowing
	1200 10 Jan	Very large and few flashes offshore	570	MC; <5 in snow southern Appalachians
7 (1997)	1200[b] 27 Jan	Overlap/small	1580[c]	AF; wave from west TX to SW MO
	0000 28 Jan	Small to medium	635	MC transition from AF; really a trough along arctic front

[a] Subjective determination of separation between freezing line and nearest ''major'' flash cluster.
[b] Denotes arctic front phase (see section 3b for definition).
[c] Ill-defined low center 12 h later; see text.

however, because it was difficult to determine which was the dominant surface low during the calculation period. The low was actually an elongated trough extending from the Midwest into Texas, collocated with an arctic front and ahead of a fast-moving surface anticyclone.

c. Stabilities and convection

Since this study focuses on lightning and therefore convection, it is important to assess not only lifting mechanisms but also environmental stability. Areas of frozen precipitation are overlain by low-level cold air masses. In such cases convection, if it exists, is frequently elevated. Colman (1990), who asserted that nearly all winter convection east of the Rocky Mountains is of the elevated variety, substantiates this occurrence. Traditional stability measures such as convective available potential energy (CAPE) and lifted index (LI) will therefore mislead, since they are calculated by lifting a low-level air parcel to its lifting condensation level. Indeed, PCGRIDDS-derived LIs were overwhelmingly positive in the 27 periods (seven cases) examined. Instead, some measure of *elevated* stability was required. Because of its ease of calculation, the measure most commonly used by forecasters is the 700–500-mb temperature difference ($-\Delta T$, in °C). The frozen precipitation areas and regions just upstream (usually southwest) were inspected to cull these ΔTs. The results are summarized in Fig. 5. For reference, the saturated adiabatic lapse in this layer is ≈19°C; a value of 20°C is nominally considered conductive to severe convection in summer and spring. Janish et al. (1996), who studied a period within our case 5, found that all CG flashes were located in regions having $-\Delta T > 17$°C (lapse rate >6.5°C km^{-1}). The average $-\Delta T$ over all available times (25) was 14.3°C. In all but three periods, values were greater than 12°C. The mean $-\Delta T$ for AF

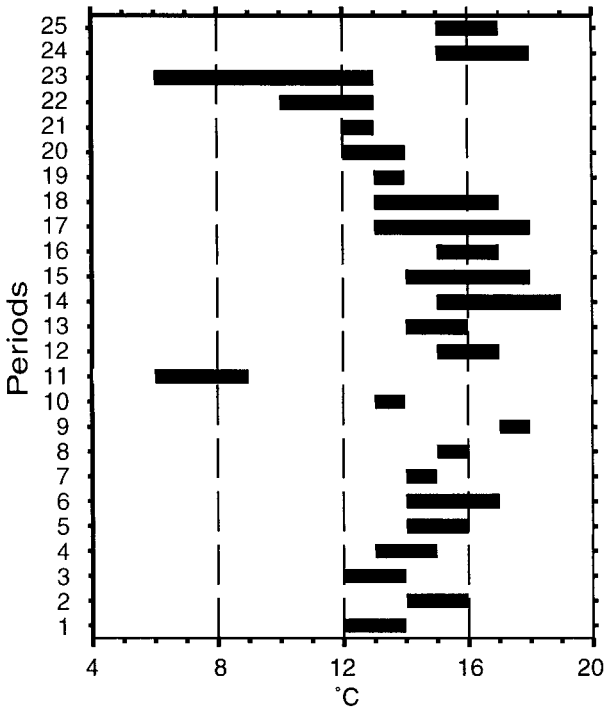

FIG. 5. Ranges of temperature differences $-\Delta T$(°C) between 700 and 500 mb, upstream and within regions impacted by heavy frozen precipitation, for 25 periods (2 periods had missing data). Mean $-\Delta T$ for available periods was 14.3.

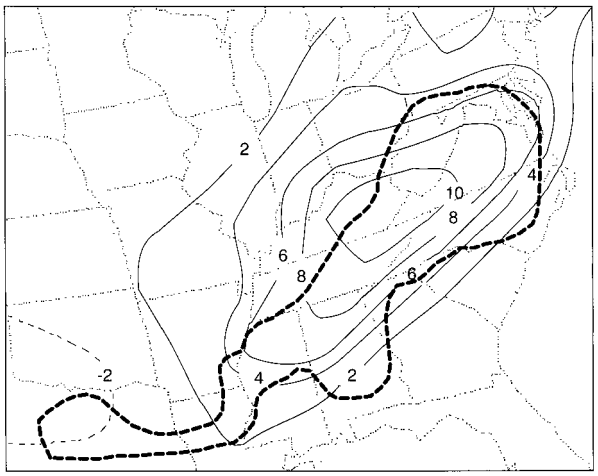

FIG. 6. Petterssen 2D frontogenesis in 10^{-10} K m^{-1} s^{-1} for 850–700-mb layer (thin solid lines), from Eta Model initialization at 1200 UTC 2 Feb 1996 (case 5). Thick dashed line envelops heavy frozen precipitation impact area on 2 Feb only (from *Storm Data*). Calculation was done with personal computer program PCGRIDDS.

phases was 14.9°C, not significantly different than the overall mean. The conclusion is that significant conditional instability existed during most periods of this study.

Slantwise convection is also possible in the cool season. This type of convection has been widely attributed to the presence of conditional symmetric instability (CSI; Bennetts and Hoskins 1979; Emanuel 1983). As demonstrated by Schultz and Schumacher (1999), CSI has seen wide misapplication for the purpose of explaining banded precipitation structures and slantwise convection. CSI, along with potential symmetric instability (PSI), are forms of moist symmetric instability (MSI). The most common method for assessing CSI, using geostrophic absolute momentum (M_g) and equivalent potential temperature (θ_e) surfaces, actually measures PSI. One must use instead the *saturated* equivalent potential temperature θ_{es} in the calculation for CSI. In saturated regions, as is usually the case with heavy frozen precipitation, $\theta_e = \theta_{es}$ and CSI and PSI are equivalent. Therefore the traditional method of calculating CSI in such regions was used, and henceforth the instability will be called MSI. Although this calculation may have some inaccuracies, as does the PCGRIDDS routine used to execute it (Schultz 2001), it remains the most widely available, simplest, and quickest method in use by NWS forecasters today.

The resulting PCGRIDDS calculations show little evidence for MSI, except for small values in case 1. Pfost (1996) also found such MSI for this case. As Schultz and Schumacher (1999) point out, however, MSI usually coexists with strong frontogenesis and *both* are required for slantwise convection. Since AF phases involve a front by definition, we investigated the existence of frontogenesis using a two-dimensional Petterssen frontogenesis calculation within PCGRIDDS. The results confirmed the existence of strong frontogenesis across the frozen precipitation impact area in most AF periods. An example is shown by Fig. 6. Such frontogenesis was usually evident in the 1000–850- or 850–700-mb layers; it was well north of the impact areas in the 700–500-mb layer. Analogously, Trapp et al. (2001) showed correspondence between an Oklahoma heavy snowfall and frontogenesis near 600 mb. Frontogenetic circulations probably provided initial lifting of a parcel in a gravitationally unstable elevated layer, previously indicated by large 700–500-mb $-\Delta T$ values. This lifting would yield upright elevated convection. Since the growth rate of such gravitational convection is greater than that of slantwise convection (Bennetts and Sharp 1982), the former should eventually dominate the latter. We believe this was so during most of the AF phases, because of scant evidence for MSI and because the aforementioned environmental stabilities were more supportive of gravitational rather than slantwise convection.

Moreover, soundings and model analyses generally showed some positive CAPE on the warm side of the surface front in AF phases. Such CAPE is typified by the sounding shown in Fig. 7. This instability supported convection that, through horizontal advection, could have influenced the microphysics of clouds in the downwind cold air mass. In such a scenario, there may be

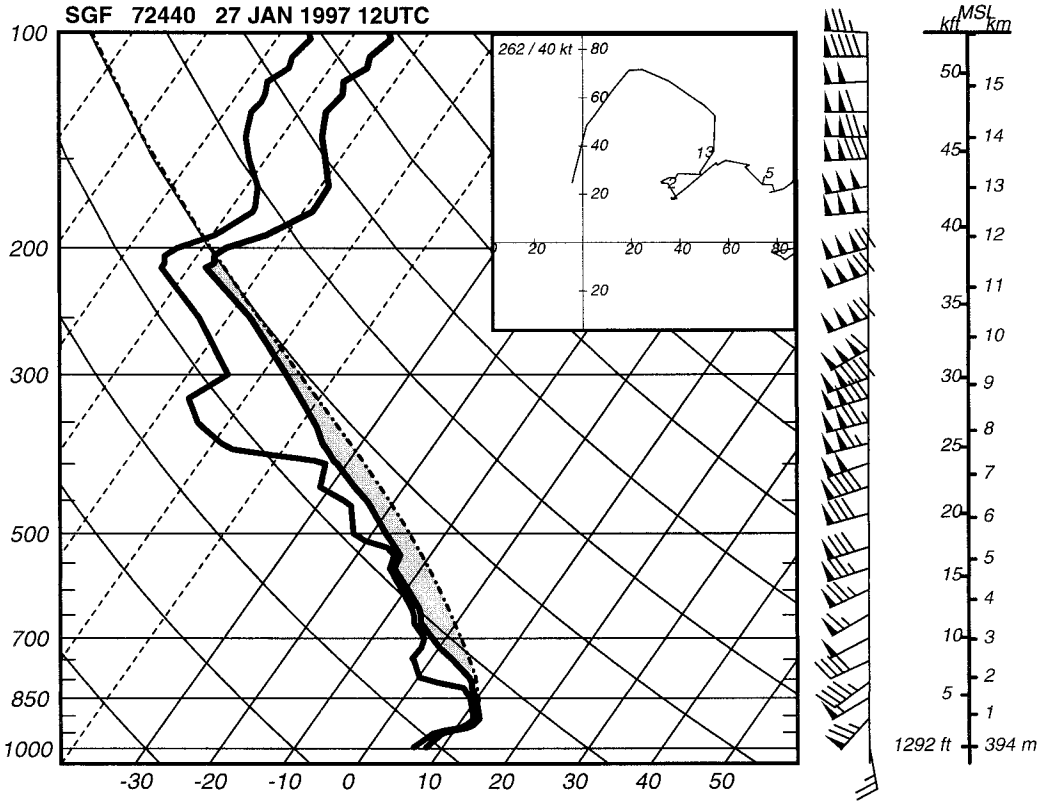

FIG. 7. Skew *T*–log*p* diagram and hodogram of upper air sounding from Springfield, MO, at 1200 UTC 27 Jan 1997 (case 7). Pressure in mb is plotted on ordinate and temperature in °C on abcissa. Wind barbs are in kt. Shaded area between the temperature curve and a moist adiabat (dash–dot curve) is positive CAPE corresponding to the most unstable parcel in the lowest 150 mb (lifted from near 850 mb). Positive CAPE for this parcel was computed to be 708 J kg^{-1}.

no need to appeal to MSI to explain the frozen precipitation.

4. Lightning and precipitation patterns

The convection, lightning, and precipitation patterns were examined for each period so as to associate the phenomena with the aforementioned synoptic patterns. This was done to investigate and develop forecast tools for frozen precipitation, using CG lightning as the main ingredient. Although some cases appeared at the outset to be unique, the 27 periods *within* the cases were chosen as the analysis units, rather than stratifying by case. This was done primarily because many cases exhibited both phase types (AF and MC).

Since the central focus of this study was the relationship between CG flashes and heavy frozen precipitation, the spatial separation between the flashes and the surface freezing line was assessed. Given that the 0°C surface isotherm forms a continuous line and that flashes yield a dataset of numerous discrete points, it is inherently difficult to derive a single representative measure of proximity between the two. Therefore we adopted the 200-km-wide buffer zone straddling the freezing line, as detailed in section 2b. This zone was laterally truncated so as not to extend beyond the region with CG flashes, forming a trapezoid. The trapezoidal shape deviated from rectangular when the freezing line was curvilinear, in which case the buffer zone width varied and the 200-km criterion could only be approximated. In all periods, the zone on the cold side of the freezing line enveloped nearly all flashes in the subfreezing surface air, in agreement with observations that convection can only extend a limited distance into a deeper, colder air mass (Holle and Cortinas 1998). In contrast, there were many CG flashes on the warm side of the freezing line but beyond the buffer zone. To eliminate these flashes from consideration, we calculated within-zone flash totals and then divided them by the total within the entire flash domain (defined in section 2b). Figures 3c and 4c provide examples of how this methodology was applied for an AF phase within case 5 (1200 UTC 2 Feb 1996) and an MC phase within case 6 (1200 UTC 9 Jan 1997).

Table 2 lists several flash calculations for each of the 27 periods. These calculations include flash totals, positive flash numbers, and percentages for the entire domain and for the buffer zone. This table should be compared to Table 1 for contemporaneous cyclone/front

TABLE 2. Cloud-to-ground flash numbers and percent positive for the domain and buffer. Analogous calculations for buffer-to-domain comparison also included. Quantities are defined by alphabetic letters and ratios in the table header row for clarity.

Case (year)	Time (UTC) and date	Total in domain (A)	Total positive in domain (B)	In-buffer total (C)	In-buffer positive (D)	% positive in domain (B/A)	% positive in buffer (D/C)	% buffer to domain (C/A)	% positive buffer to domain (D/B)
1 (1994)	0000* 10 Feb	371	121	326	106	33	33	88	88
	1200* 10 Feb	1812	141	733	87	8	12	40	62
	0000* 11 Feb	1435	292	199	39	20	20	14	13
	1200 11 Feb	5229	215	5	4	4	80	0.1	2
2 (1995)	0000** 6 Jan	48	2	0	0	4		0	0
	1200 6 Jan	5410	1151	4070	955	21	23	75	83
	0000 7 Jan	15 415	3647	87	58	24	67	0.5	2
	1200 7 Jan	9012	1228	0	0	14		0	0
3 (1995)	0000 4 Feb	1870	341	36	16	18	44	2	5
	1200 4 Feb	2330	915	971	486	39	50	42	53
	0000 5 Feb	368	261	0	0	71		0	0
4 (1996)	1200 1 Jan	7858	1376	0	0	17		0	0
	0000 2 Jan	1168	193	0	0	17		0	0
	1200 2 Jan	636	91	2	2	14	100	0.3	2
	0000 3 Jan	13 652	2378	32	9	17	28	0.2	0.4
5 (1996)	0000* 2 Feb	990	87	713	61	9	9	72	70
	1200* 2 Feb	24 453	3521	19 385	3342	14	17	79	95
	0000 3 Feb	5334	1169	1570	530	22	34	29	45
	1200 3 Feb	3346	764	704	209	23	30	21	27
	0000** 4 Feb	314	24	16	7	8	44	5	29
6 (1997)	1200 8 Jan	4255	662	0	0	16		0	0
	0000 9 Jan	9345	2021	28	15	22	54	0.3	0.7
	1200 9 Jan	2459	444	0	0	18		0	0
	0000 10 Jan	1728	524	0	0	30		0	0
	1200 10 Jan	47	24	3	2	51	67	6	8
7 (1997)	1200* 27 Jan	170	67	169	66	39	39	99	99
	0000 28 Jan	26 058	5105	12 366	2276	20	18	47	45

* Denotes arctic front phases (see section 3b for definition).
** Only 3 h available for computation.

characteristics. Perhaps the most important column in Table 2 is the second from the right, which gives the percentage of total flashes in the domain that were in the buffer zone (C/A). This is a measure of the magnitude of convection near the subfreezing surface air mass. The periods with single asterisks in the date/time column are those deemed to be AF phases. These periods are characterized by high flash percentages in the buffer zone. Figure 3c illustrates the flash pattern of one such period, in case 5. The buffer percentages in this case decreased with time, as a wave formed on the front and became a migratory cyclone. Contrast this with Fig. 4c, which illustrates an MC phase. In this period, there was a large horizontal separation between the freezing line and the flashes, which were in the warm sector of a deep cyclone centered in Massachusetts. Only 12 h earlier, this cyclone was 1200 km away in Kentucky.

There were two periods with large in-buffer-zone percentages that were associated with unambiguous migratory cyclones. The first, 1200 UTC 6 January 1995 in case 2, had 75% of total flashes within the buffer zone. Closer inspection of the surface data reveals that the flashes were indeed near the surface freezing isotherm where it took a southward dip into Arkansas. Some of this dip (but not all of it) may be attributed to cooler temperatures in the higher terrain of the Ozark Mountains. Although the cyclone was deepening, there was no front in the area. Therefore we cannot entirely explain the flash proximity to the cold air in this case. The second MC period with numerous buffer zone flashes, 1200 UTC 4 February of case 3, had 42% of flashes in the buffer zone. Further examination revealed that the majority of flashes were offshore, over the Gulf Stream. It is likely that warm moist air in this area contributed to the instability needed to produce convection near the freezing line in Maryland and New Jersey, as suggested by the climatological study of Orville (1990).

Although the in-buffer-zone percentages are useful quantifiers of the influence of convection on downwind frozen precipitation, they may be diminished by large flash numbers *outside* that zone (the denominator of the fraction). In such cases, one should also take into account the *absolute* flash numbers within the zone, which is listed in the fifth column (C) of Table 2. To assess possible influences of the convection on the frozen precipitation in a subjective way, it is desirable to know the distance from that precipitation to the nearest significant cluster of CG flashes. The need for such additional characterizations, however, is somewhat obviated by averaging of all AF and MC periods. These averages expose a clear distinction between lightning

patterns in the two types of synoptic settings. The mean buffer-to-domain flash percentage for MC periods was 10% and for AF periods 65%.

Table 2 also presents analogous results for flashes delivering positive charge to ground. There were unusually high values of percent positive in the domain (B/A) and in the buffer zone (D/C), averaging for all nonzero periods 22% and 40%, respectively. Compare these percentages to Orville and Silver's (1997) mean winter figure of around 5%. One of our early hypotheses was that there would be a bipole pattern of flash polarity (Orville et al. 1988), with a predominance of positive flashes at the northern end of the bipole, near the subfreezing air. Although not an explicit measure of the spatial separation of positive and negative flash locations, one might expect the bipole pattern to be reflected in the rightmost column D/B of Table 2. This column contains the percentage of the domain's positive flashes located in the buffer zone. The column shows nine periods with percentages greater than 40, of which five were AF periods. Nevertheless, corresponding figures in the column to the left, the *total* flashes in the buffer zone versus domain (C/A), reveal that those figures and the ones from D/B are highly correlated (correlation coefficient $r = 0.97$). That is, when a large percentage of *total* domain flashes were within the buffer zone, a large percentage of the domain's *positive* flashes were also within that zone. Thus no spatial segregation between those positive flashes and *negative* ones may be inferred. This was also the subjective conclusion from inspection of numerous CG flash location and buffer zone maps. This inspection also revealed no *temporal* trend toward a bipole pattern.

5. Discussion

Seven major winter storms affecting the southeast United States were examined for synoptic and lightning patterns. During these storms, 27 12-h periods were subjectively categorized as either an arctic front type or migratory cyclone type. The type depended on the nature of the relevant cyclones and fronts. Many of the seven storms had a transition from AF to MC with time; in such circumstances it is more appropriate to describe the types as phases.

The MC phase (21 of 27 periods) involved a deepening or mature cyclone, with typical strong cyclonic advection and S-shaped deformation of thickness and resulting fronts. With few exceptions (section 4), major lightning clusters in MC phases were distant (>150 km) from the surface freezing line and well into the warm sector of the cyclone. The convection producing these flashes was most likely upright, based at the surface, and growing in an air mass of substantial CAPE.

The AF phase was less common (6 of 27 periods) but had more connection between lightning and precipitation. Flashes were isolated in a 200-km-wide buffer zone that straddled the surface freezing line. All but one of the AF phases had a high percentage (>40%) of its storm total flashes within the buffer zone (Table 2, column C/A). Four of the six periods had a significant number of flashes in the subfreezing surface air, near the heavy frozen precipitation. Such patterns indicate a strong relationship between convection and that precipitation.

Heaviest *ice* (not snow) accumulations were produced in cases 1, 5, 6, and 7 (Fig. 1, second column). Remaining cases produced mainly snow or lighter ice accumulations. All but one of the heavy ice cases (case 6) had AF periods. The large accumulations appeared to occur during quasi-steady lift over an entrenched arctic air mass. This is reasonable from a forecasting perspective, since slow-moving systems usually produce the most precipitation. Ice accumulation in the exceptional case 6 was due instead to persistent cold air damming in the lee of the Appalachians.

The generation and maintenance of convection in the AF phase is not as clear as in the MC phase. The AF phases are typified by prolonged synoptic-scale lifting of warm moist air over arctic air, which supports elevated convection. Such convection appears to only extend a limited distance into cold air north of the front since it becomes increasingly separated from warm unstable air. Nevertheless, sufficient CAPE exists in the warm air just south of the surface front to support upright surface-based gravitational convection there. Under strong southwest flow aloft, ice crystals from the tops of such convection are evidently advected over stratiform clouds on the cold side of the front. This situation resembles the ''seeder–feeder'' mechanism (Bergeron 1950; Hobbs et al. 1980; Houze 1993) where crystals fall from the seeder zone aloft into the stratiform feeder zone below, where the crystals grow by deposition and possibly by riming.

The AF pattern, despite its apparent infrequency, poses a disproportionate threat of damaging frozen precipitation in the southeast United States. Once a forecaster becomes aware that such a synoptic pattern has evolved, flash data can help diagnose and forecast heavy frozen precipitation. The forecaster should be alert to a high flash density within 100 km on either side of the surface freezing line, particularly if there are significant numbers of flashes on the cold side of that line. Such a configuration signals that convection—elevated, surface based, or slantwise—is probably active in producing ice crystals for seeding stratiform clouds below in the cold air. Such a process has the potential for generating heavy snow or ice accumulations.

6. Summary

Seven storm cases in the southeastern United States were examined that produced both heavy frozen precipitation at the surface and CG lightning associated with the storm. The cases were known to have both phenomena, but their relationships and extents were

largely unknown prior to the study. Synoptic- and regional-scale environments, aloft and at the surface, were assessed. Particular attention was paid to situations when lightning was within 200 km of the surface freezing line and was near frozen precipitation.

The following are results of the study:

- Most cases had a split flow pattern in the upper troposphere, with distinct southern and northern branches of the polar jet stream. The southern branch jet stream had southwesterly winds and was instrumental in the development of frozen precipitation in the study area. The two jet streams tended to phase as the storm matured.
- Most cases possessed significant elevated instability, with 700–500-mb temperature differences averaging more than 14°C.
- Two types of surface phases were distinguished, arctic fronts and migratory cyclones.
- In AF phases, strong frontogenesis was found near the arctic front in the 1000–850- and 850–700-mb layers. We believe that such frontogenesis contributed to the upward motion that produced the frozen precipitation.
- During AF phases, significant numbers of CG flashes were in or near subfreezing surface air and frozen precipitation. Strong southwest flow aloft likely advected ice particles from convection over lower stratiform clouds, seeding them and causing heavy frozen precipitation.
- Three of the seven cases included AF phases, but in all of these cases these phases changed into MC phases.
- During MC phases, CG flashes were more likely to be in the warm sector of the surface cyclone and away from the surface freezing line.
- There was no evidence for a bipole pattern of CG flashes.
- Forecasters in the southeast United States should pay particular attention to the AF phase. During this phase, frequent CG flashes near the surface freezing line may indicate significant accumulations of frozen precipitation downwind in the subfreezing surface air.

Acknowledgments. We thank Kurt Hondl and Karen Cooper of NSSL for help with lightning and radar software, and David Schultz of NSSL for input on MSI and his review of this paper. Eric Thaler of NWS Denver composed the frontogenesis calculation in PCGRIDDS. This work was supported by a Partners grant from the Cooperative Program for Operational Meteorology, Education and Training.

REFERENCES

Bennetts, D. A., and B. J. Hoskins, 1979: Conditional symmetric instability—A possible explanation for frontal rainbands. *Quart. J. Roy. Meteor. Soc.,* **105,** 945–962.

——, and J. C. Sharp, 1982: The relevance of conditional symmetric instability to the prediction of mesoscale frontal rainbands. *Quart. J. Roy. Meteor. Soc.,* **108,** 595–602.

Bergeron, T., 1950: Uber der mechanisms der ausgiebigen Nedershlage. *Ber. Dtsch. Wetterdienstes,* **12,** 225–232.

Bradshaw, T., 1994: Relationships between conditional symmetric instability, thunder, and heavy snowfall during the ''storm of the century.'' National Weather Service Southern Region Tech. Attachment SR/SSD 94-21, Fort Worth, TX, 8 pp.

Brook, M., M. Nakano, and P. R. Krehbiel, 1982: The electrical structure of Hokoriku winter thunderstorms. *J. Geophys. Res.,* **87,** 1207–1215.

Colman, B. R., 1990: Thunderstorms above frontal surfaces in environments without positive CAPE. Part I: A climatology. *Mon. Wea. Rev.,* **118,** 1103–1121.

Cummins, K. L., M. J. Murphy, E. A. Bardo, W. L. Hiscox, R. B. Pyle, and A. E. Pifer, 1998: A combined TOA/MDF technology upgrade of the U.S. National Lightning Detection Network. *J. Geophys. Res.,* **103,** 9035–9044.

Dickinson, M. J., L. F. Bosart, W. E. Bracken, G. J. Hakim, D. M. Schultz, M. A. Bedrick, and K. R. Tyle, 1997: The March 1993 superstorm cyclogenesis: Incipient phase synoptic- and convective-scale flow interaction and model performance. *Mon. Wea. Rev.,* **125,** 3041–3072.

Emanuel, K. A., 1983: Conditional symmetric instability: A theory for rainbands within extratropical cyclones. *Mesoscale Meteorology—Theories, Observations and Models,* D. K. Lilly and T. Gal-Chen, Eds., Reidel, 231–245.

Goto, Y., K. Narita, H. Komuro, and N. Honma, 1992: On the characteristics of winter lightning and thundercloud. *Proc. Int. Conf. on Lightning and Static Electricity,* Atlantic City, NJ, FAA Rep. DOT/FAA/CT-92/20, 57-1–57-5.

Gurka, J. J., E. P. Auciello, A. F. Gigi, J. S. Waldstreicher, K. K. Keeter, S. Businger, and L. G. Lee, 1995: Winter weather forecasting throughout the eastern United States. Part II: An operational perspective of cyclogenesis. *Wea. Forecasting,* **10,** 21–41.

Hobbs, P. V., T. J. Matejka, P. H. Herzegh, J. D. Locatelli, and R. A. Houze Jr., 1980: The mesoscale and microscale structure and organization of clouds and precipitation in midlatitude cyclones. I: A case study of a cold front. *J. Atmos. Sci.,* **37,** 568–596.

Holle, R. L., and A. I. Watson, 1996: Lightning during two central U.S. winter precipitation events. *Wea. Forecasting,* **11,** 599–614.

——, and J. V. Cortinas Jr., 1998: Thunderstorms observed at surface temperatures near and below freezing across North America. Preprints, *19th Conf. on Severe Local Storms,* Minneapolis, MN, Amer. Meteor. Soc., 705–708.

——, R. E. Lopez, K. W. Howard, K. L. Cummins, M. D. Malone, and E. P. Krider, 1997: An isolated winter cloud-to-ground lightning flash causing damage and injury in Connecticut. *Bull. Amer. Meteor. Soc.,* **78,** 437–441.

Houze, R. A., 1993: *Cloud Dynamics.* Academic Press, 573 pp.

Janish, P. R., C. A. Crisp, J. V. Cortinas, R. L. Holle, and R. H. Johns, 1996: Development of an ingredients based approach to forecasting hazardous winter weather in an operational environment. Preprints, *15th Conf. on Weather Analysis and Forecasting,* Norfolk, VA, Amer. Meteor. Soc., 56–59.

Keeter, K. K., and J. W. Cline, 1991: The objective use of observed and forecast thickness values to predict precipitation type in North Carolina. *Wea. Forecasting,* **6,** 456–469.

Kocin, P. J., and L. W. Uccellini, 1990: *Snowstorms along the Northeastern Coast of the United States: 1955 to 1985. Meteor. Monogr.,* No. 44, Amer. Meteor. Soc., 280 pp.

——, P. N. Schumacher, R. F. Morales Jr., and L. W. Uccellini, 1995: Overview of the 12–14 March 1993 superstorm. *Bull. Amer. Meteor. Soc.,* **76,** 165–182.

Moore, P. K., and V. P. Idone, 1999: Cloud-to-ground lightning at low surface temperatures. *11th Int. Conf. on Atmospheric Electricity,* Guntersville, AL, NASA/CP-1999-209261, 472–475.

Mote, T. L., D. W. Gamble, S. J. Underwood, and M. L. Bentley, 1997: Synoptic-scale features common to heavy snowstorms in the southeast United States. *Wea. Forecasting,* **12,** 5–23.

Orville, R. E., 1990: Winter lightning along the East Coast. *Geophys. Res. Lett.,* **17,** 713–715.

——, 1993: Cloud-to-ground lightning in the blizzard of '93. *Geophys. Res. Lett.,* **20,** 1367–1370.

——, and A. C., Silver, 1997: Lightning ground flash density in the contiguous United States: 1992–95. *Mon. Wea. Rev.,* **125,** 631–638.

——, R. W. Henderson, and L. F. Bosart, 1988: Bipole patterns revealed by lightning locations in mesoscale storm systems. *Geophys. Res. Lett.,* **15,** 129–132.

Pfost, R. L., 1996: Disastrous Mississippi ice storm of 1994. *Natl. Wea. Dig.,* **20,** 15–33.

Roohr, P. B., and T. H. Vonder Haar, 1996: Lightning in winter storm convection: Initial findings and examination of 5 Mar 1990 Colorado ''storm of the century.'' Preprints, *15th Conf. on Weather Analysis and Forecasting,* Norfolk VA, Amer. Meteor. Soc., 64–67.

Rooney, J. F., 1967: The urban snow hazard in the United States: An appraisal of disruption. *Geogr. Rev.,* **57,** 538–559.

Schultz, D. M., 1999: Lake-effect snowstorms in northern Utah and western New York with and without lightning. *Wea. Forecasting,* **14,** 1023–1031.

——, cited 2001: Calculating CSI. [Available online at http://www.nssl.noaa.gov/~schultz/csi/contents/calc.shtml.]

——, and P. N. Schumacher, 1999: The use and misuse of conditional symmetric instability. *Mon. Wea. Rev.,* **127,** 2709–2732; Corrigendum, **128,** 1573.

Studwell, A. M., and R. E. Orville, 1995: Characteristics of cloud-to-ground lightning in a severe winter storm, 9–12 February 1994. Preprints, *Sixth Conf. on Aviation Weather Systems,* Dallas, TX, Amer. Meteor. Soc., 176–181.

Trapp, R. J., D. M. Schultz, A. V. Ryzhkov, and R. L. Holle, 2001: Multiscale structure and evolution of an Oklahoma winter precipitation event. *Mon. Wea. Rev.,* **129,** 486–501.

Uccellini, L. W., and P. J. Kocin, 1987: Interaction of jet streak circulation during heavy snow events along the east coast of the United States. *Wea. Forecasting,* **2,** 289–308.

Williams, E. R., 1988: Anomalous electrification in winter storms. Preprints, *15th Conf. on Severe Local Storms,* Baltimore, MD, Amer. Meteor. Soc., 304–308.